J BONE ONCOL 52 (2025) 100684

Contents lists available at ScienceDirect

Journal of Bone Oncology

journal homepage: www.elsevier.com/locate/jbo

Research Paper

The phosphatase CTDSPL2 promotes proliferation, invasion, metastasis and regorafenib resistance in osteosarcoma

Guannan Bai [a,1], Shaobo Zhao [a,1], Manli Zhao [b,1], Limiao Chen [c], Wenhao Chen [a,*]

[a] Department of Orthopedics, Children's Hospital, Zhejiang University School of Medicine, National Children's Regional Medical Center, National Clinical Research Center for Child Health, 3333 Binsheng Road, Hangzhou, Zhejiang Province 310052, China
[b] Department of Pathology, Children's Hospital, Zhejiang University School of Medicine, National Children's Regional Medical Center, National Clinical Research Center for Child Health, 3333 Binsheng Road, Hangzhou, Zhejiang Province 310052, China
[c] Children's Hospital, Zhejiang University School of Medicine, National Children's Regional Medical Center, National Clinical Research Center for Child Health, 3333 Bingsheng Road, Hangzhou, Zhejiang Province 310052, China

HIGHLIGHTS

- A systemic screen using regorafenib-treated osteosarcoma cell lines.
- CTDSPL2 was found significantly up-regulated in regorafenib-treated osteosarcoma cell lines.
- CTDSPL2 promoted osteosarcoma cell proliferation, invasion and metastasis while suppressing apoptosis in vitro.
- CTDSPL2 was significantly up-regulated in osteosarcoma tissues compared with adjacent tissues.
- CTDSPL2 is a potential therapeutic target for patients with osteosarcoma.

ARTICLE INFO

Keywords:
Osteosarcoma
Regorafenib
CTDSPL2
Apoptosis
Proliferation
Invasion
Metastasis

ABSTRACT

Osteosarcoma is the most common bone malignancy in children and adolescents. Patients with metastatic and recurrent osteosarcoma have poor prognosis. Regorafenib is a multi-kinase inhibitor recommended as a complement to standard chemotherapy in the treatment of advanced osteosarcoma. The mechanisms associated with regorafenib resistance remains unclear.

In this study we performed transcriptomics, proteomics and phosphorylated proteomics using regorafenib-treated osteosarcoma cell lines (MG-63, HOS-MNNG for transcriptomics, HOS-MNNG for proteomics and phosphorylated proteomics). After comprehensive multiomics and verification analyses of differentially expressed genes, essential genes for the malignancy of osteosarcoma cells were identified. The effects of essential genes on the proliferation, invasion, and migration of osteosarcoma were determined. The study also evaluated their role in the apoptosis of osteosarcoma cells. The up-regulation of essential genes was determined by immunohistochemistry assays.

Using comprehensive multiomics and verification analyses we found that the CTDSPL2 gene might play a role in the malignancy and Regorafenib resistance in osteosarcoma. In vitro and clinical specimen assays demonstrated that CTDSPL2 promotes the proliferation, invasion and metastasis of osteosarcoma cells, while inhibiting tumor cell apoptosis.

In conclusion CTDSPL2 was identified as an essential gene for survival of osteosarcoma cells. Knockdown of CTDSPL2 expression significantly inhibited the proliferation, invasion, and metastasis of osteosarcoma cells, suggesting that it is involved in the formation and development of osteosarcoma tumors. Our data showed that CTDSPL2 is a potential therapeutic target for patients with osteosarcoma.

* Corresponding author.
E-mail address: whchenortho@zju.edu.cn (W. Chen).
[1] These authors contributed equally to this work.

https://doi.org/10.1016/j.jbo.2025.100684
Received 4 February 2025; Received in revised form 16 April 2025; Accepted 22 April 2025
Available online 26 April 2025

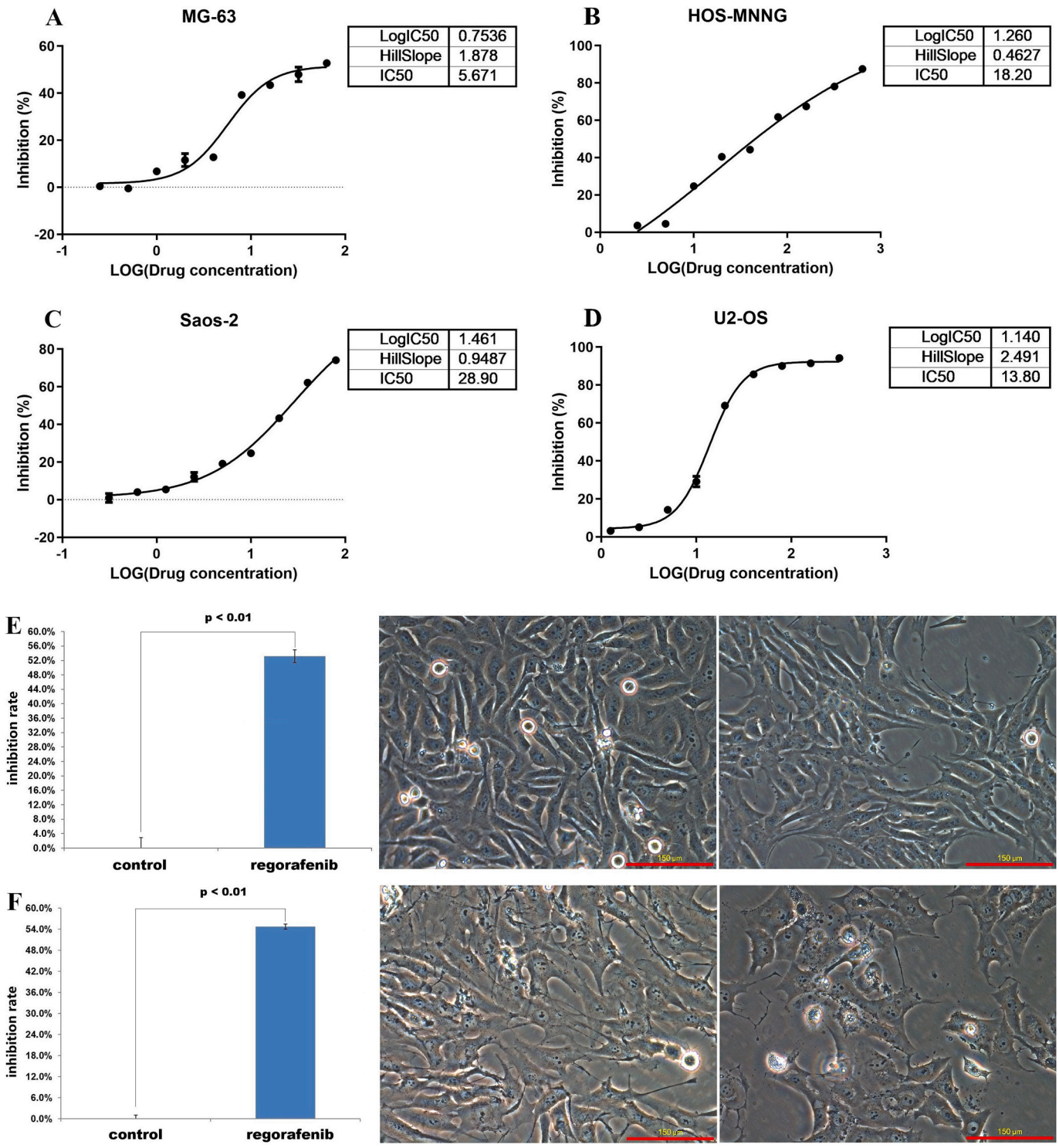

Fig. 1. IC50 and MTT assays in four well-known osteosarcoma cell lines. The half maximal inhibitory concentration (IC50) assays were performed in four well-known osteosarcoma cell lines. A. HOS-MNNG; B. Saos-2; C. MG-63; D. U2-OS. MTT assays were performed in two osteosarcoma cell lines. E. HOS-MNNG; F. MG-63. Scale bar: 150 μm.

1. Introduction

Osteosarcoma is the most common bone malignancy found in children and adolescents worldwide [1]. Tumor resection and chemotherapy using a combination of cisplatin, doxorubicin, and methotrexate are the primary treatments for osteosarcoma [2]. Eighty percent of patients are presumed to have clinically undetectable micrometastases at diagnosis [3]. Those who do not respond well to chemotherapy have a poor prognosis. A 5-year survival rate of approximately 20 % is observed in patients with metastatic and recurrent osteosarcoma, which has remained virtually unchanged for the last three decades [4].

The increased knowledge of the molecular biology of oncogenesis, angiogenesis, and the tumor microenvironment has resulted in clinical trials of multi-kinase inhibitors for treatment of refractory osteosarcoma [5–8]. Regorafenib is a multi-kinase inhibitor that targets kinases in tumor cells (KIT, RET, RAF-1, BRAF, and BRAFV600E), the vasculature

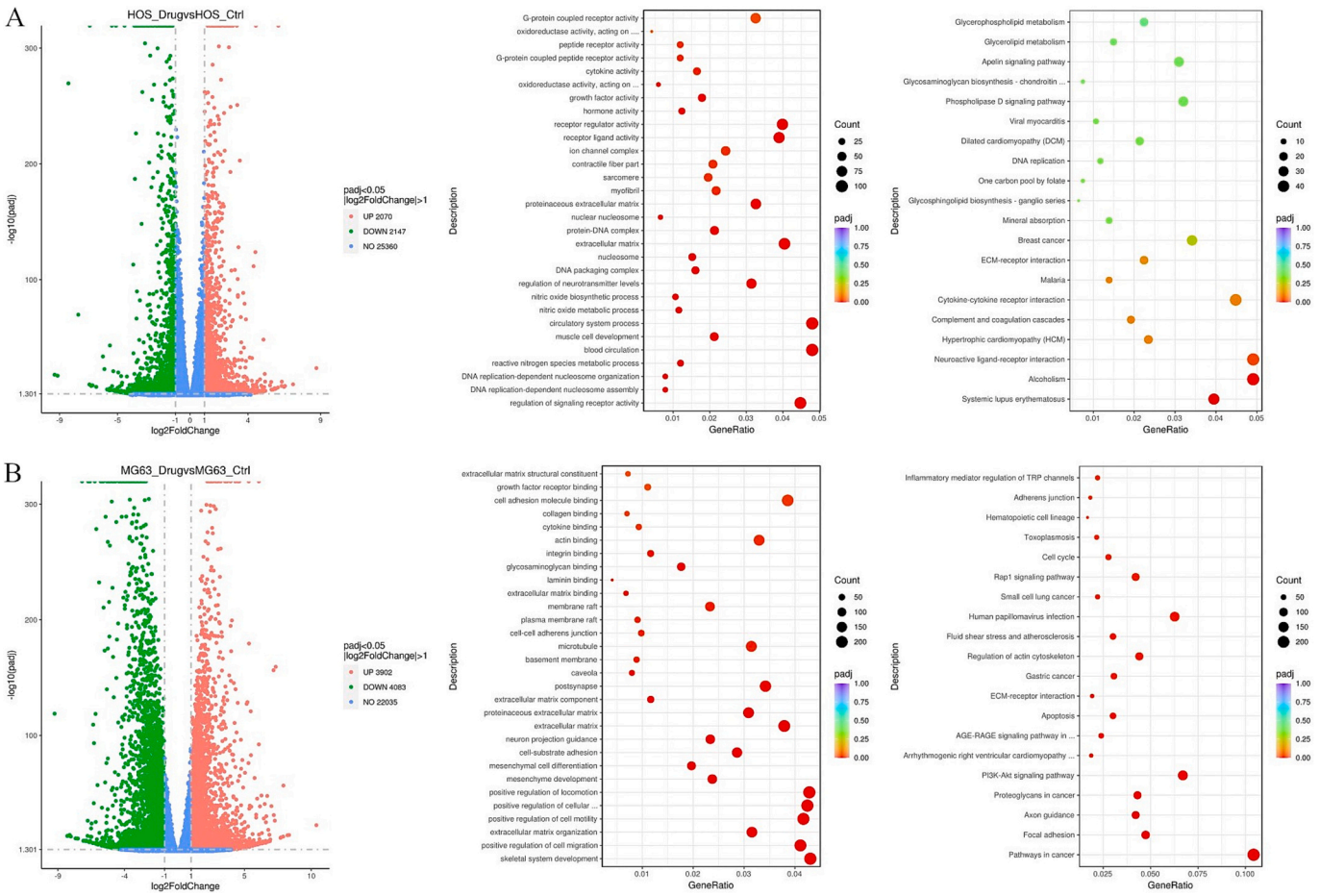

Fig. 2. Differentially expressed genes (DEGs) in transcriptomic analyses and GO/KEGG pathways. A. HOS-MNNG, regorafenib treated vs. control; B. MG-63, regorafenib treated vs. control.

(VEGFR-1, VEGFR-2, VEGFR-3, and TIE2), and the tumor microenvironment (PDGFR and FGFR) [9]. However, marginal effects were documented in the phase 2 trial of regorafenib, and regorafenib was recommended only as an agent complementary to standard chemotherapy in the treatment of advanced osteosarcoma [6]. The mechanisms of regorafenib resistance, that play an important role in the limited therapeutic effect in treating osteosarcoma, remains unclear. Understanding these mechanisms may benefit the discovery of novel therapeutic targets for patients with osteosarcoma.

In this study, we performed a systemic screening of regorafenib-treated osteosarcoma cell lines; MG-63, HOS-MNNG for transcriptomics and HOS-MNNG for proteomics and phosphorylated proteomics. After comprehensive multiomics and verification analyses of differentially expressed genes (DEGs), we found that CTDSPL2 was significantly up-regulated in regorafenib-treated osteosarcoma cell lines, and we speculate whether CTDSPL2 plays a role in regorafenib resistance in osteosarcoma. Knock-down of CTDSPL2 showed the gene is a factor in promoting osteosarcoma cell proliferation, invasion, and metastasis while suppressing apoptosis in osteosarcoma cells in vitro. In osteosarcoma tumor tissue samples CTDSPL2 was significantly up-regulated in compared with normal adjacent tissues. Our results show that CTDSPL2 is a potential therapeutic target for patients with osteosarcoma tumors.

2. Materials and methods

2.1. Cell culture

The cell lines HOS-MNNG, Saos-2, MG-63 and U2-OS were obtained from ATCC (American Type Culture Collection). HOS-MNNG, Saos-2, MG-63 and U2-OS cells were cultured in DMEM (Gibco) containing 10 % fetal bovine serum (FBS, BI, Kibbutz Beit Haemek, Israel), 100 U/mL penicillin and 0.1 mg/mL streptomycin (BBI Life Sciences, Shanghai, China) at 37 °C in a humidified incubator with 5 % CO_2.

2.2. CCK-8 assay

Cells were seeded into 96-well plates (2×10^4 cells/well) and cultured for 24 h, 48 h, and 72 h.

Four hours before absorbance measurement, 10 μL CCK-8 solution was added. The absorbance was measured at 450 nm with a microplate reader after incubation at 37 °C for 2 h.

2.3. MTT assay

Cells were plated at a density of 3×10^4 cells in a 96-well plate for 24 h, and after the 80 % confluence was reached, cells were treated with 0.1 % DMSO, which was used as a vehicle for 24 h. Cells were stained with MTT (0.5 mg/mL), and then the percent of viability were quantified by absorbance value (OD) at 570 nm. The MTT agents were purchased from Sigma Chemical Co.

2.4. Generation of regorafenib-treated cell lines

Regorafenib-treated sublines were derived from the HOS-MNNG and MG-63 parental cell lines by exposure to regorafenib (Bayer AG 73–4506) following initial dose–response studies of regorafenib (0 μM to 64 μM) over 48 h from which IC50 values were obtained. Based on these

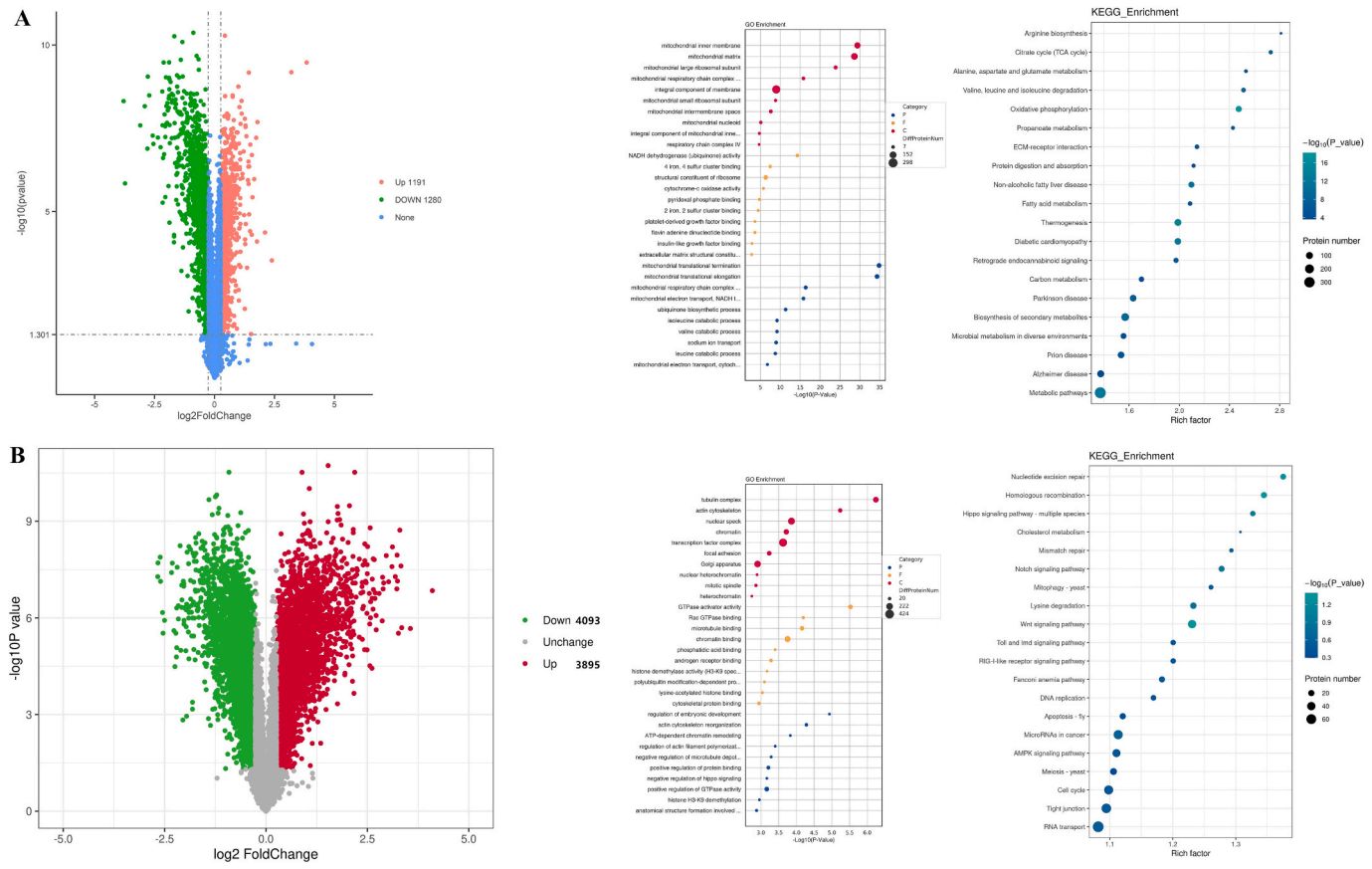

Fig. 3. Differentially expressed genes (DEGs) in proteomic and phosphorylated proteomic analyses and GO/KEGG pathways in regorafenib treated HOS-MNNG cell line and control. A. proteomic analyses; B. phosphorylated proteomic analyses.

results, we utilized the optimal dose (25 μM) and time (48 h) of regorafenib treatment for the following transcriptomic and proteomic studies. We performed the MTT assay for in both HOS-MNNG and MG-63 cell lines incubated in regorafenib at the above-mentioned concentration and time.

2.5. Transcriptomics and analyses

Four paired samples from the regorafenib-treated HOS-MNNG cell line and control group and four samples from the regorafenib-treated MG-63 cell line and control group underwent transcriptomic analyses. After RNA quantification and qualification, a total amount of 1 μg RNA per sample was used as input material for the RNA sample preparations. Sequencing libraries were generated using the NEBNext® UltraTM RNA Library Prep Kit for Illumina® (NEB, USA) following the manufacturer's recommendations, and index codes were added to attribute sequences to each sample. Briefly, mRNA was purified from total RNA using poly-T oligo-attached magnetic beads. Fragmentation was carried out using divalent cations under elevated temperature in NEBNext First Strand Synthesis Reaction Buffer (5X). First-strand cDNA was synthesized using random hexamer primers and M−MuLV Reverse Transcriptase (RNase H). Second strand cDNA synthesis was performed using DNA Polymerase I and RNase H. The remaining overhangs were converted into blunt ends via exonuclease/polymerase activities. After adenylation of the 3′ ends of DNA fragments, NEBNext adaptors with hairpin loop structures were ligated to prepare for hybridization. To preferentially select cDNA fragments 250 ~ 300 bp in length, the library fragments were purified with the AMPure XP system (Beckman Coulter, Beverly, USA). Then, 3 μl USER Enzyme (NEB, USA) was used with size-selected, adaptor-ligated cDNA at 37 °C for 15 min followed by 5 min at 95 °C before PCR. Then, PCR was performed with Phusion High-Fidelity DNA polymerase, universal PCR primers and Index (X) Primer. Finally, PCR products were purified (AMPure XP system), and library quality was assessed on the Agilent Bioanalyzer 2100 system. Generation System using TruSeq PE Cluster Kit v3-cBot-HS (Illumina) according to the manufacturer's instructions. After cluster generation, the library preparations were sequenced on an Illumina NovaSeq platform, and 150 bp paired-end reads were generated.

2.6. Proteomic and phosphorylated proteomic analyses

Four paired samples from the regorafenib-treated HOS-MNNG cell line and control group were subjected to transcriptomic analyses. After sample preparation, SDS–PAGE separation and filter-aided sample preparation, 100 μg peptide mixture of each sample was labeled using TMT reagent according to the manufacturer's instructions (Thermo Fisher Scientific). TMT-labeled peptides were fractionated by RP chromatography using the Agilent 1260 infinity II HPLC. The peptide mixture was diluted with buffer A (10 mM HCOONH4, 5 % ACN, pH 10.0) and loaded onto an XBridge Peptide BEH C18 Column, 130 Å, 5 μm, 4.6 mm X 100 mm column. The peptides were eluted at a flow rate of 1 ml/min with a gradient of 0 %–7 % buffer B (10 mM HCOONH4, 85 % ACN, pH 10.0) for 5 min, 7–40 % buffer B for 5–40 min, 40 %–100 % buffer B for 45–50 min, and 100 % buffer B for 50–65 min. The elution was monitored at 214 nm based on the UV light trace, and fractions were collected every 1 min for 5–50 min. The collected fractions were combined into 10 fractions and dried via vacuum centrifugation at 45 °C.

LC–MS/MS analysis was performed on an Orbitrap Exploris 480 mass spectrometer (Thermo Fisher Scientific) that was coupled to Easy nLC (Thermo Fisher Scientific) for 60/90 min (determined by project proposal). The mass spectrometer was operated in positive ion mode. MS data were acquired using a data-dependent top10 method dynamically

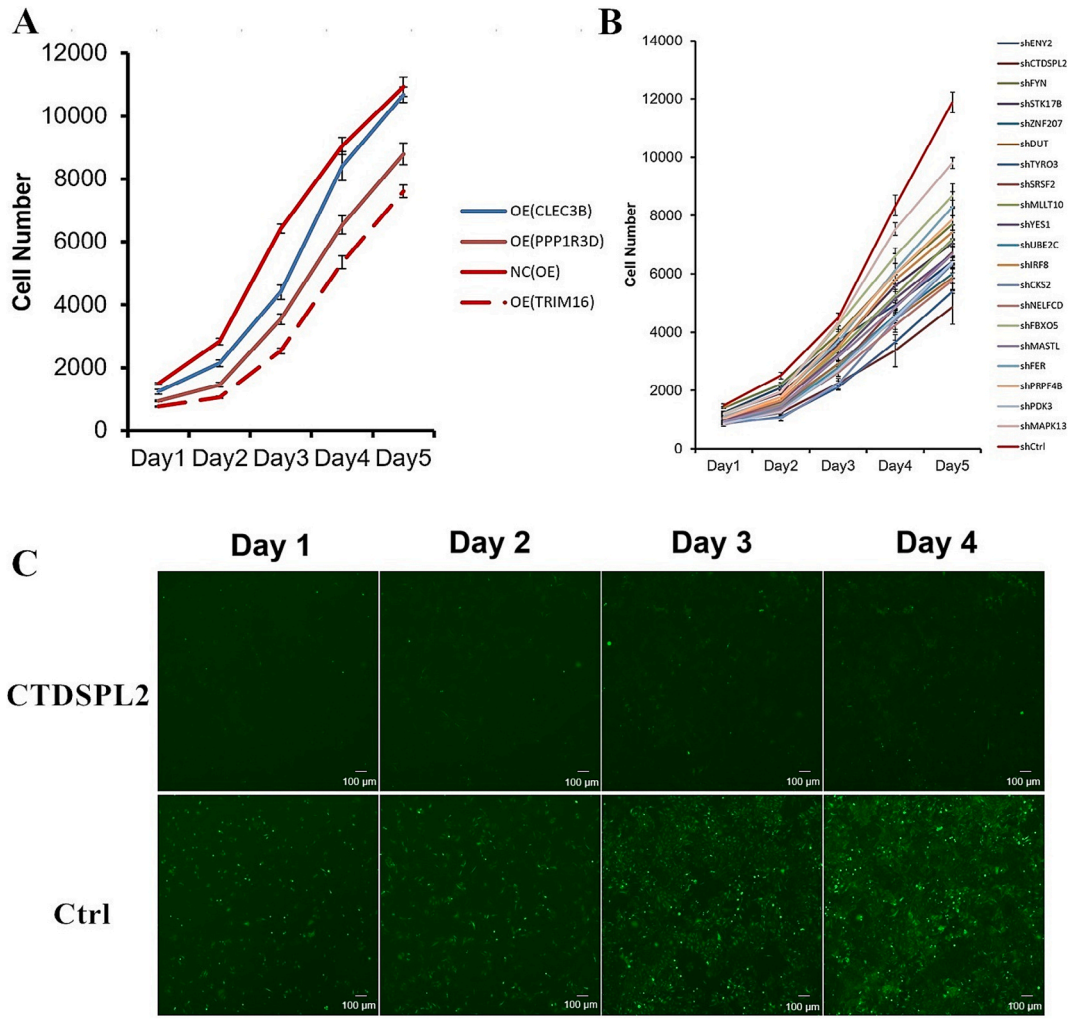

Fig. 4. Determination of the candidate gene involved in the malignancy of osteosarcoma. 20 genes were either knocked down (for the up-regulated genes) or over-expressed (for the down-regulated genes) in the HOS-MNNG cell line based on their expression in the omics, then cell proliferation rates were measured. A. overexpression of the down-regulated genes; B. down-regulation of the up-regulated genes; C. cell proliferation was inhibited in CTDSPL2 knockdown group, compared with control group. Scale bar: 100 μm.

choosing the most abundant precursor ions from the survey scan (350–1800 *m/z*) for HCD fragmentation. Survey scans were acquired at a resolution of 120,000 at *m/z* 200 with an AGC target of 3e6 and a maxIT of 50 ms. MS2 scans were acquired at a resolution of 45,000 for HCD spectra at *m/z* 200 with an AGC target of 2e5 and a maxIT of 45 ms, and the isolation width was 2 *m/z*. Only ions with a charge state between 2–6 and a minimum intensity of 2e3 were selected for fragmentation. Dynamic exclusion for selected ions was 30 s. The normalized collision energy was 30 eV.

2.7. Data analyses

Differential expression analysis of two groups (two biological replicates per condition) was performed using the DESeq2 R package (1.16.1). DESeq2 provides statistical routines for determining differential expression in digital gene expression data using a model based on the negative binomial distribution. The resulting P values were adjusted using Benjamini and Hochberg's approach for controlling the false discovery rate. Genes with an adjusted p value < 0.05 found by DESeq2 were considered differentially expressed. MS/MS raw files were processed using the MASCOT engine (Matrix Science, London, UK; version 2.6) embedded into Proteome Discoverer 2.2 and searched against the UniProt_HomoSapiens_20394_20210127 database. The search parameters included trypsin as the enzyme used to generate peptides with a maximum of two missed cleavages permitted. A precursor mass tolerance of 10 ppm was specified and 0.05 Da tolerance for MS2 fragments. Except for TMT labels, carbamidomethyl (C) was set as a fixed modification. Variable modifications were oxidation (M), acetyl (protein N-term), phospho(ST), and phospho(Y). A peptide and protein false discovery rate of 1 % was enforced using a reverse database search strategy. Proteins with fold change >1.2 and adjusted p value (Student's *t* test) < 0.05 were considered differentially expressed proteins. Phosphopeptides with a fold change > 1.2 and an adjusted p value (Student's *t* test) < 0.05 were considered differentially expressed phosphopeptides.

2.8. Gene enrichment analysis

The Database for Annotation, Visualization and Integrated Discovery (DAVID) database can provide the biological consequences for gene expression (https://david. abcc. Ncifc rf. gov/). In this study the KEGG pathway and GOBP enrichment analyses of identified DEGs were performed using the DAVID database.

2.9. shRNA transfection

The sequence of shRNAs targeting CTDSPL2 was cloned and inserted

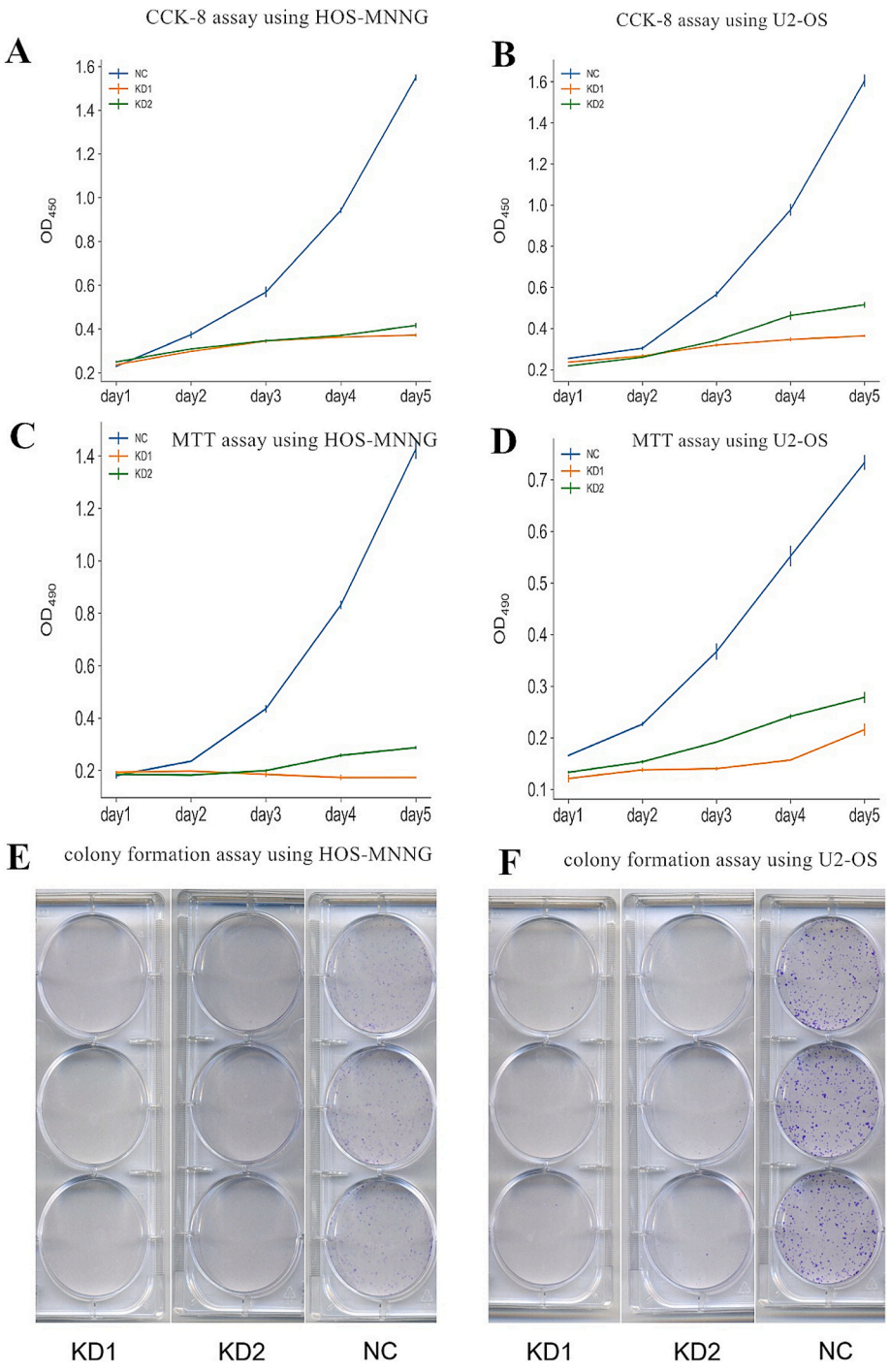

Fig. 5. CTDSPL2 promoted osteosarcoma cell proliferation. A. CCK-8 assay using HOS-MNNG cell line; B. CCK-8 assay using U2-OS cell line; C. MTT assay using HOS-MNNG cell line; D. MTT assay using U2-OS cell line; E. colony formation assay using HOS-MNNG cell line, KD1, KD2 and control from left to right; F. colony formation assay using U2-OS cell line. KD1: shRNA1 group; KD2: shRNA2 group; NC: control group.

into the pLVX vector. The sequence of CTDSPL2 shRNA1 was 5′-CCTGGAACGAATGTCTCAGAT-3′; the sequence of CTDSPL2 shRNA2 was 5′- CGGAGTAGAATTGAACGTGAT-3′. Transfection was performed using Lipofectamine 2000 (Invitrogen, Carlsbad, CA, USA) according to the manufacturer's guidelines.

2.10. Colony-forming assays

The shRNA-transfected cells and controls were cultured in DMEM supplemented with 10 % fetal bovine serum. For colony formation assays, equal numbers of cells from each individual clone were plated onto 12-well plates. Colonies were visualized after 10 d. The cells were washed with PBS, fixed in 4 % paraformaldehyde for 5 min, and again washed with PBS. Fixed cells were stained with 0.05 % crystal violet in distilled water for 1 h, washed with distilled water and then drained. Images of stained colonies were scanned using an Epson scanner (GT9700F; Tokyo, Japan) and then counted with Image-Pro Plus 5.1 software (Media Cybernetics). The experiments were repeated in triplicate.

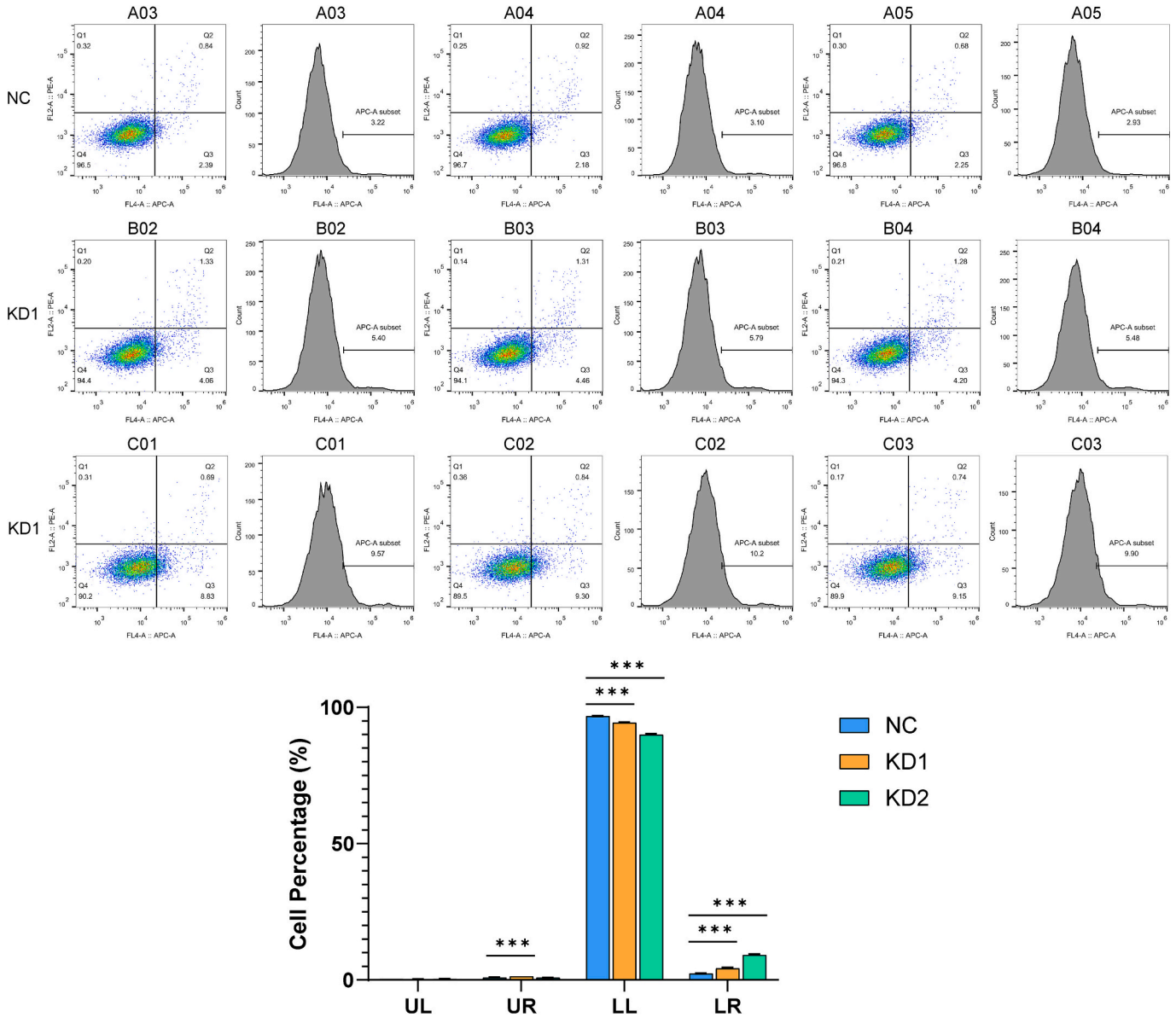

Fig. 6. CTDSPL2 inhibited the apoptosis of osteosarcoma cells. Annexin V/PI staining and flow cytometry was performed to measure the percentages of live cells, viable apoptotic cells, late apoptotic cells and dead cells. UL: upper left quadrant, represents dead cells; UR: upper right quadrant, represents late apoptotic cells; LL: lower left quadrant, represents live cells; LR: lower right quadrant, represents viable apoptotic cells. KD1: shRNA1 group; KD2: shRNA2 group; NC: control group.

2.11. Transwell assay

For the cell invasion assay, we used transwell cell culture chambers (BD Biosciences, Franklin Lakes, NJ, USA) with 8 mm pore size (Illipore, Billerica, MA, USA), coated with 50 μL of BD Matrigel matrix on polyethylene terephthalate (PET) membranes. Cells were trypsinized, resuspended in serum-free medium, and plated in the upper chamber of the transwell. The lower chamber was filled with 90 % McCoy's 5a medium plus 10 % FBS. Cells invasion proceeded at 37 °C for 48 h. After removing the nonmigrating cells the cells invading the PET membrane were fixed (4 % formaldehyde/PBS) and stained with 0.5 % crystal violet. After staining, the bottom of the membrane were photographed and invading cell counted under a bright field microscope at × 100. Five random fields were counted per membrane.

2.12. Annexin V/PI staining

Briefly, shRNA-transfected cells and control cells were split and added to 6-well plates. After 36 h, the cells were treated with pimozide for 24 h. Thereafter, the cells were trypsinized and suspended in ice-cold phosphate-buffered saline (PBS). For Annexin V/PI staining, flow cytometry was performed using dead.

The Cell apoptosis kit with Annexin V FITC and PI solution from Thermo Fisher Scientific (Waltham, MA) according to the manufacturer's instructions. The results were analyzed with FlowJo software.

2.13. RNA isolation and RT-qPCR

Total RNA was extracted from HOS-MNNG and U2-OS cells using TRIzol (Invitrogen, CA, USA) and was reverse transcribed with an mRNA reverse transcription kit (Takara, Japan). Specific primers for RT–qPCR were used to detect the mRNA expression of CTDSPL2. All primers were

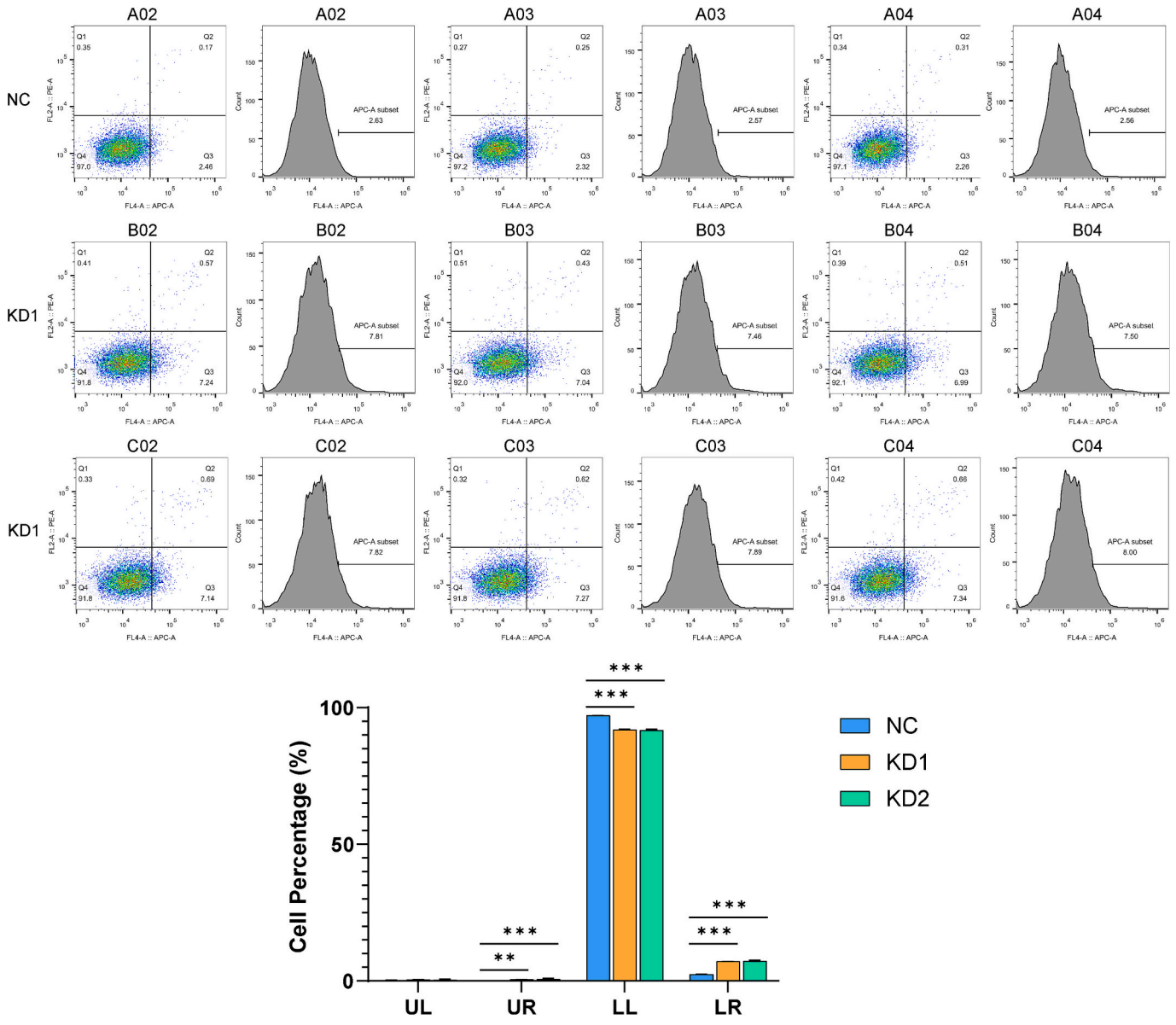

Fig. 6. (*continued*).

synthesized by Sangon Biotech (Shanghai, China). CTDSPL2-forward primer 5′- GGTGACGGTGCTTGACTA −3′ and CTDSPL2-reverse primer 5′- GATTTCAACCGGAACAATA −3′. The ACTB primers were: ACTB −forward primer 5′- GCGTGACATTAAGGAGAAGC −3′ and ACTB −reverse primer 5′- CCACGTCACACTTCATGATGG −3′. Relative quantification was performed by the 2-ΔΔCt method.

2.14. Western blot

Cells were lysed with the RIPA lysis buffer from Roche Ltd (Basel, Switzerland) containing protease inhibitors. The protein concentration in the lysates was measured by a Micro BCA Protein Assay Kit (Pierce Biotechnology, IL, US). Samples were separated by 10 % SDS–PAGE then transferred to Amersham Protran nitrocellulose membranes (GE Healthcare Life Sciences, Fairfield, USA). The nitrocellulose membranes were incubated with primary antibodies for the target proteins CTDSPL2 and GAPDH (Proteintech, Wuhan, China) at dilutions of 1:1000 and 1:5000 for 2 h, respectively. The proteins were detected and quantified using the Odyssey® CLx Infrared Imaging System (LI-COR Biosciences, NE, USA).

2.15. Immunohistochemistry

We conducted immunohistochemical staining analysis to measure the protein expression of CTDSPL2 in osteosarcoma tissues and adjacent normal tissues according to standard immune-peroxidase staining procedure. Paraffin-embedded tissues were sliced into 4 μm sections, deparaffinized, then blocked with avidin/biotin for 20 min. The slides were incubated with primary antibodies overnight at 4 °C. Next, the slides were treated with secondary antibody (Invitrogen) and HRP conjugate for 1 h and then developed with DAB (Invitrogen). Finally, the slides were counterstained with hematoxylin. The IHC staining results of CTDSPL2 were independently evaluated by two pathologists.

2.16. Statistical analysis

All values are expressed as the mean ± SEM (standard error of measurement). Data were analyzed using an unpaired two-tailed *t* test. The statistical significance was indicated as p value < 0.05.

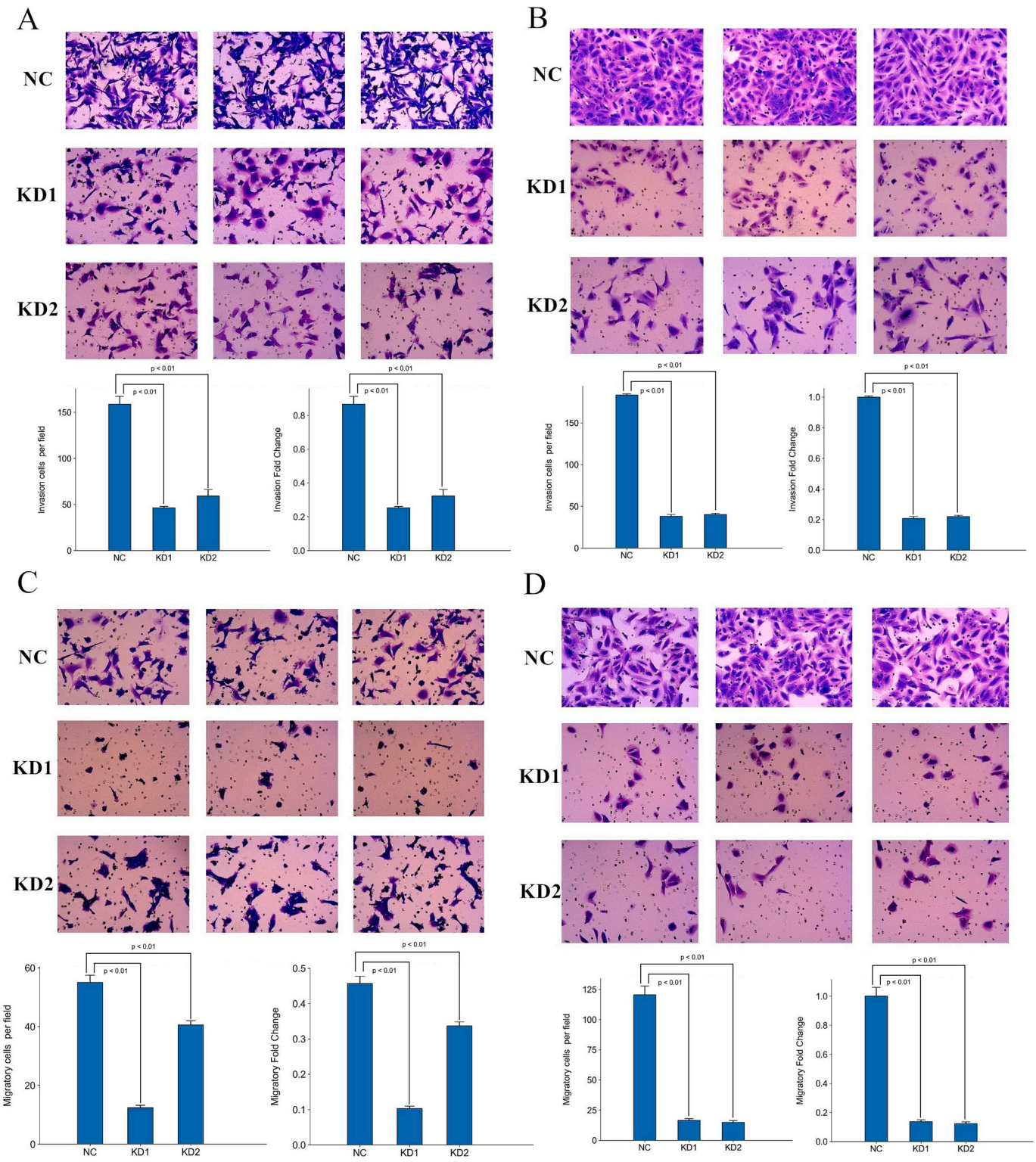

Fig. 7. CTDSPL2 promoted the invasion and metastasis of osteosarcoma cells. A. invasion chamber assay using HOS-MNNG cell line; B. invasion chamber assay using U2-OS cell line; C. Transwell assay using HOS-MNNG cell line; D. Transwell assay using U2-OS cell line. KD1: shRNA1 group; KD2: shRNA2 group; NC: control group.

3. Results

3.1. HOS-MNNG and MG-63 cell lines were selected to perform the transcriptomic and proteomic analyses

We analyzed regorafenib-treated cell lines for transcriptomic and proteomic changes. The half maximal inhibitory concentration (IC50) of regorafenib was determined using the MTT viability assay for four well-known osteosarcoma cell lines; MG-63, HOS-MNNG, Saos-2, and U2-OS (Fig. 1A-D). Based on these results we used the optimal dose (25 μM) and time (48 h) of regorafenib treatment for the following transcriptomic and proteomic studies. We performed the MTT assay to evaluate the

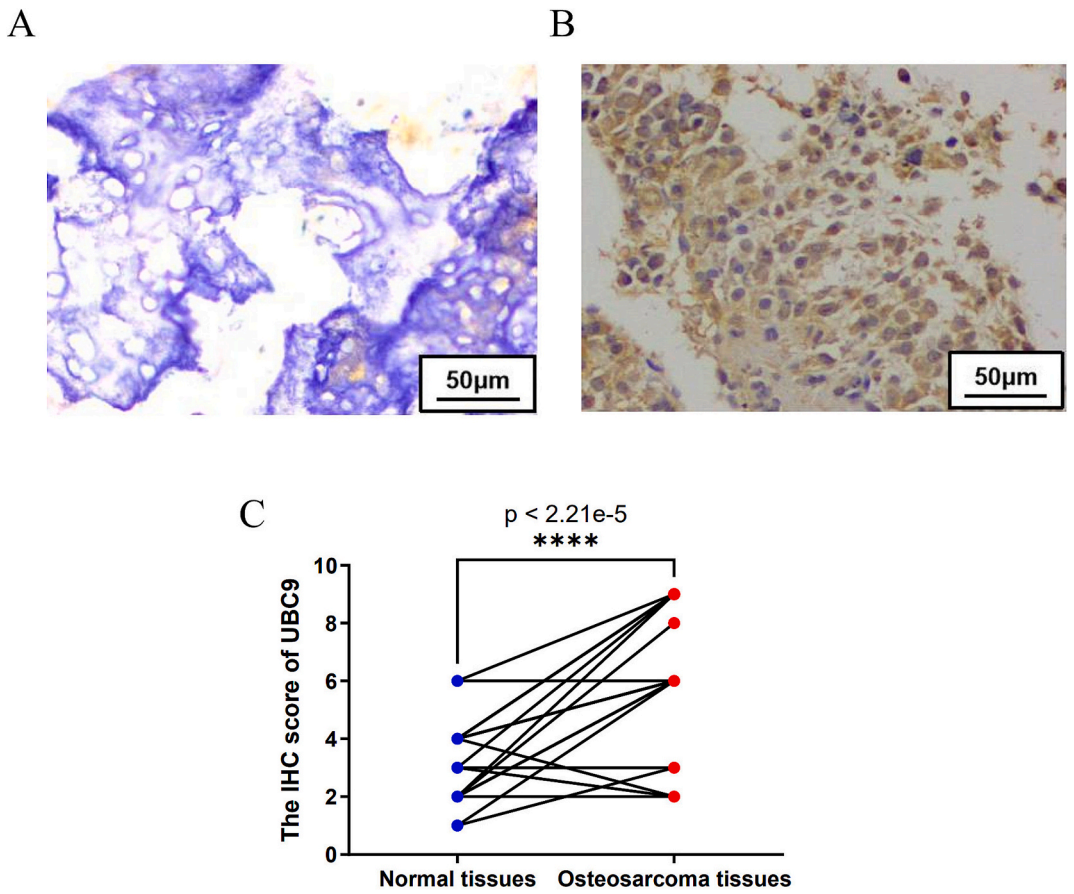

Fig. 8. CTDSPL2 was up-regulated in osteosarcoma tissues. Representative IHC images of CTDSPL2 protein expression in Normal tissues (A) and osteosarcoma tissues (B) (×200 magnification). (C). IHC score for CTDSPL2 in osteosarcoma patients. ***p < 0.001 Scale bar: 50 μm.

effect of regorafenib on both HOS-MNNG and MG-63 cell lines. Cell viability was significantly decreased after regorafenib treatment compared to untreated control cells (Fig. 1E-F).

3.2. Differentially expressed genes were identified in the regorafenib-treated cell lines

We next determined the DEGs in osteosarcoma cells after treatment with regorafenib. We chose two cell lines, i.e., HOS-MNNG and MG-63, and treated them with 25 mM regorafenib for 48 h and conducted transcriptomic analyses. Regorafenib-treated HOS-MNNG cells also underwent proteomic and phosphorylated proteomic analyses. Transcriptomic analyses identified 4217 DEGs in the HOS-MNNG cell line, 2147 up-regulated genes and 2070 down-regulated genes. In the MG-63 cell line 7985 DEGs were identified, including 4083 upregulated genes and 3902 downregulated genes (Fig. 2). Proteomic analyses of regorafenib treated HOS-MNNG cell identified 2471 differentially expressed proteins, including 1191 up-regulated proteins and 1280 down-regulated proteins (Fig. 3). In the phosphorylated proteomic analyses 7988 differentially expressed peptides were identified, 3895 up-regulated peptides and 4093 down-regulated peptides (Fig. 3). Gene Ontology (GO) annotation and KEGG pathway annotation were performed and after these comprehensive analyses 20 genes were found to be differentially expressed in all omics analyses (Figs. 2-3).

3.3. CTDSPL2 was determined to be the candidate gene involved in the malignancy of osteosarcoma

Based on their expression in the omics analysis these 20 genes were either knocked down (for the up-regulated genes) or over-expressed (for the down-regulated genes) in the HOS-MNNG cell line to determine their function. The influence on the cell proliferation rate were documented as the fold change in cell count (control/interference) on day-5 after shRNA infection. A fold change ≥ 1.5 was not observed with the knock down of three over-expressed genes (Fig. 4A). A fold change of ≥ 1.5 was observed in knockdown two genes, ENY2 and CTDSPL2 (Fig. 4B). After additional single target validation, CTDSPL2 was determined to be a candidate gene involved in the malignancy of osteosarcoma (Fig. 4C).

3.4. CTDSPL2 promoted osteosarcoma cell proliferation

To determine whether CTDSPL2 promoted the proliferation of osteosarcoma cells, we first generated CTDSPL2 knockdown cell lines KD1 and KD2 in HOS-MNNG cells and KD1 and KD2 in U2-OS cells. A colony formation assay was performed and the colonies were counted after eight days of cell culture. Both CCK-8 and MTT viability assays were performed five days after plating. There were significantly fewer colonies in the KD1 and KD2 constructs than in the control groups in both HOS-MNNG and U2-OS lines ($p < 0.05$). Proliferation was significantly lower in KD1 and KD2 cells of both in HOS-MNNG and U2-OS cell lines compared with the controls ($p < 0.05$, Fig. 5). These results suggest that CTDSPL2 positively affects the proliferation of osteosarcoma cells.

3.5. CTDSPL2 inhibited the apoptosis of osteosarcoma cells

Apoptosis is a cell death pathway that can be triggered by chemotherapy. We assessed the role that CTDSPL2 might play in the regorafenib associated resistance to apoptosis of osteosarcoma cells. The CTDSPL2 knockdown cell lines were assayed for the percentages of live cells, viable apoptotic cells, late apoptotic cells, and dead cells using

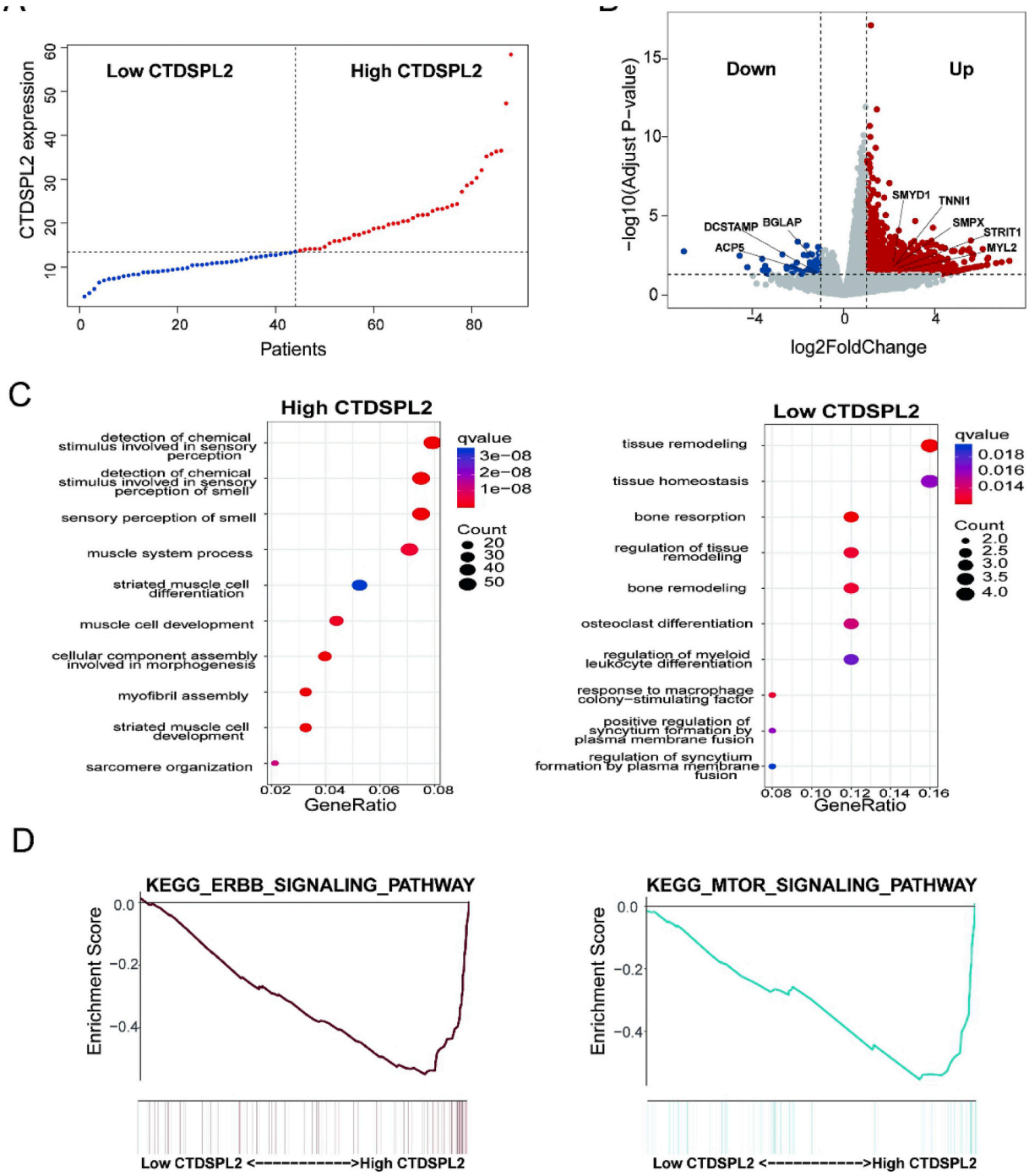

Fig. 9. Potential mechanisms about the role of CTDSPL2 on proliferation, invasion and metastasis of osteosarcoma cells. (A) Within the TARGET-OS, we divided 88 patients into a high expression group and a low expression group based on the median value of CTDSPL2 expression; (B) DEGs between the two groups were identified; (C) (D) Functional analysis was performed.

flow cytometry. For the HOS-MNNG cell lines (Fig. 6A), the percentage of dead cells in KD1 was significantly higher than that in the control group ($p < 0.05$) and there was no significant difference in the percentage of dead cells between the KD2 and control groups ($p > 0.05$). The percentages of viable and late apoptotic cells were significantly lower in both the KD1 and KD2 groups than in the control group ($p < 0.05$). For the U2-OS cell lines (Fig. 6B), no increase in the percentage of dead cells in the KD1 and KD2 knock downs was observed ($p > 0.05$). However, the percentages of viable and late apoptotic cells were similarly lower in both KD1 and KD2 cells than in the control group ($p < 0.05$). These data suggest that CTDSPL2 inhibited the apoptosis of osteosarcoma cells, which might be one of the mechanisms of regorafenib resistance in osteosarcoma tumors.

3.6. *CTDSPL2 promoted the invasion and metastasis of osteosarcoma cells*

We performed invasion chamber assays for both of the CTDSPL2 knockdown cell lines. We observed significantly lower cell invasion rates in KD1 and KD2 knock downs of both HOS-MNNG and U2-OS cell lines compared with the control group ($p < 0.05$, Fig. 7). To explore whether CTDSPL2 promoted the invasion and metastasis of

osteosarcoma cells we conducted Transwell chamber assays. We observed significantly lower cell migration rates in KD1 and KD2 knock downs of both HOS-MNNG and U2-OS cell lines compared with the control group ($p < 0.05$, Fig. 7). These data suggest that CTDSPL2 promoted the invasion and metastasis of osteosarcoma cells.

3.7. CTDSPL2 was up-regulated in osteosarcoma tissues

We selected osteosarcoma tissues and adjacent tissues from five different patients to determine whether CTDSPL2 was up-regulated in the tumor tissue. Immunohistochemistry assays illustrated that the number of CTDSPL2-positive cells was significantly higher in osteosarcoma tissues than in adjacent tissues, suggesting that CTDSPL2 was highly expressed in osteosarcoma ($p < 0.05$, Fig. 8).

3.8. Potential mechanisms about the role of CTDSPL2 on proliferation, invasion and metastasis of osteosarcoma cells

Within the TARGET-OS, we divided 88 patients into a high expression group and a low expression group based on the median value of CTDSPL2 expression, DEGs between the two groups were identified and functional analysis was performed. The results showed that the highly expressed genes in the high expression group were significantly enriched in biological processes related to muscle formation, while the low expressed genes were related to bone tissue remodeling. KEGG analyses showed ErbB and mTOR pathways were involved in the CTDSPL2 induced malignancy of osteosarcoma (Fig. 9).

4. Discussion

Carboxyl-terminal domain phosphatase-like protein 2 (CTDSPL2), also known as SCP4 or HSPC129, is a metal-dependent serine/threonine phosphatase [10]. CTDSPL2 is usually located in the heterochromatin of the nucleus [11,12]. The translocation of CTDSPL2 from the nucleus to the cytosol occurs in certain circumstances [12]. Previous studies demonstrated that CTDSPL2 interacts with a variety of proteins involved in hepatic gluconeogenesis, differentiation of osteoblasts, and mesenchymal-epithelial transition [11,13,14]. The role of CTDSPL2 in most malignant tumors is largely unknown, even though CTDSPL2 has been shown to be a key player in tumor cell proliferation, invasion, and metastasis in pancreatic cancer [15]. The role of CTDSPL2 in osteosarcoma has not been explored. In this study, we identified CTDSPL2 as an essential gene involved in promoting osteosarcoma cell proliferation, invasion, and metastasis, and clinical specimens from patients with osteosarcoma implied similar results.

Regorafenib is a multikinase inhibitor targeting oncogenesis, tumor angiogenesis, and the tumor microenvironment. It has been recommended for the treatment of a variety of malignant tumors, including glioblastoma, metastatic colorectal cancer, advanced gastrointestinal stromal tumors, and hepatocellular carcinoma [16–24]. Regorafenib has also shown antitumor activity in metastatic or advanced osteosarcoma in a phase II study [6,25]. However, the antitumor effects of regorafenib were limited in osteosarcoma patients. It has been reported that induction of IL-6Rα by ATF3 enhances regorafenib resistance in hepatocellular carcinoma [26]. There is a paucity of previous studies to clarify whether regorafenib resistance plays a role in unfavorable outcomes for osteosarcoma patients treated with regorafenib. Discovering the underlying mechanism of potential regorafenib resistance in osteosarcoma is of great importance. For this, we performed transcriptomic, proteomic, and phosphorylated proteomic analyses in regorafenib-treated cell lines. The DEGs in osteosarcoma after treatment with regorafenib were acquired. Twenty genes were found to be differentially expressed in all omics analyses. After further verification, we eventually determined that the candidate CTDSPL2 gene could be involved in the malignancy of osteosarcoma.

To determine whether CTDSPL2 promoted the malignant behaviors of osteosarcoma cells, we tested cell proliferation, invasion, and migration rates in CTDSPL2 knockdown cell lines. We observed that cell proliferation, invasion, and migration were significantly depressed in CTDSPL2 knockdown HOS-MNNG and U2-OS cell lines. These data suggested that CTDSPL2 promoted the proliferation, invasion, and metastasis of osteosarcoma cells. Furthermore, we assessed whether CTDSPL2 contributed to the inhibition of osteosarcoma cell apoptosis, which may play a role in regorafenib resistance. Generally, we observed an increase in the percentage of dead cells and a decrease in the percentage of viable and late apoptotic cells, which implied that CTDSPL2 suppressed apoptosis of osteosarcoma cells. Additionally, immunohistochemistry assays illustrated that CTDSPL2 was highly expressed in osteosarcoma. These findings are consistent with those reported by Xiao et al. [15], although their results were discovered in pancreatic cancer, while ours was found in osteosarcoma. Winans et al. [27] also showed that CTDSPL2 promoted cell immortalization, migration and survival in B-cell lymphomas, which also supported our findings. As we discussed above, CTDSPL2 is a serine/threonine phosphatase. Phosphatase dysregulation occurs in cancer development [28] and many phosphatases are promising targets for anticancer treatment [29,30]. In this study, we further suggested that CTDSPL2 prolonged tumor cell survival by suppressing cell apoptosis. To the best of our knowledge there is no previous literature regarding the role of CTDSPL2 in malignant tumors.

The KEGG analyses showed the ErbB and mTOR pathways are involved in the CTDSPL2 induced malignancy of osteosarcoma. The ErbB protein family participates in tumor cell proliferation, apoptosis, motility, and metastasis. ErbB kinase overexpression correlates with a poor cancer prognosis. Evidence shows EGFR and HER2 are receptors expressed in osteosarcoma tissues and cells, while HER4 is in the nuclear compartment. Given that ErbB signaling elicits downstream signals via PI3K/Akt and MAPK impacting tumor survival, metastasis, and drug resistance, aberrant ErbB signaling may constitute a major factor in the invasive/metastatic potential of osteosarcoma. The mammalian target of rapamycin (mTOR) is a protein kinase belonging to the PI3K-related kinase family. mTOR expression is much higher in osteosarcoma (OS) tissues than in normal bone. Overactivation of mTOR signaling promotes progression of various cancers including OS. Excess mTOR activity supports tumor growth by promoting cell cycle, proliferation, and inhibiting autophagy via affecting protein synthesis. Multiple elements of the mTOR pathway are associated with OS; S6K1, 4EBP1, and eIF4E, overexpressed in OS, are downstream of activated mTOR and can promote OS cell transformation and a poor prognosis.

Taken together, our data shows that CTDSPL2 is a critical regulator of the malignant behaviors of osteosarcoma. Decreased expression of CTDSPL2 induced the suppression of cell proliferation, invasion, and migration and subsequently enhanced osteosarcoma cell apoptosis, which may contribute to regorafenib resistance. This investigation suggests that CTDSPL2 could be a potential therapeutic target for osteosarcoma and possibly other types of cancers as well.

CRediT authorship contribution statement

Guannan Bai: Writing – review & editing, Writing – original draft, Validation, Methodology, Investigation, Formal analysis, Data curation. **Shaobo Zhao:** Writing – review & editing, Writing – original draft, Validation, Methodology, Investigation, Formal analysis, Data curation. **Manli Zhao:** Visualization, Validation, Software, Resources, Methodology, Investigation. **Limiao Chen:** Visualization, Validation, Software, Resources, Methodology, Investigation. **Wenhao Chen:** Writing – review & editing, Writing – original draft, Visualization, Validation, Supervision, Software, Resources, Project administration, Methodology, Investigation, Funding acquisition, Formal analysis, Data curation, Conceptualization.

Funding

This work was supported by the grants from National Natural Science Foundation of China (82372668), the National Science Foundation for Young Scientists of China (82001312), Special Fund for the Incubation of Young Clinical Scientist, Children's Hospital of Zhejiang University School of Medicine (CHZJU2022YS008) and the Medical Innovation Foundation of Fujian Province (2021CXA032).

Declaration of competing interest

The authors declare that they have no known competing financial interests or personal relationships that could have appeared to influence the work reported in this paper.

Acknowledgements

N/A.

Ethics Statement

The study was approved by the Research Ethics Committee of Children's Hospital of Zhejiang University School of Medicine (2022-IRB-109) and complied with the Helsinki Declaration. Written informed consent was obtained from the patient's parents/legal guardian for publication and any accompanying images.

Availability of data and material.

The datasets used and/or analyzed during the current study are available from the corresponding author on reasonable request.

Authors' contributions

W.C. designed the experiments and directed the study jointly. G.B., S. Z., and L.C. performed the experiments. M.Z. evaluated the clinical specimens by immunohistochemistry. G.B., S.Z., and M.Z. analyzed the data and generated the figures. W.C. provided critical design and analysis support. G.B. and W.C. wrote the manuscript.

References

[1] J. Huang, S.C. Chan, C.H. Ngai, et al., Global incidence, mortality and temporal trends of cancer in children: a joinpoint regression analysis, *Cancer Med.* 12 (2) (2023) 1903–1911.
[2] P.G. Casali, S. Bielack, N. Abecassis, et al., Bone sarcomas: ESMO–PaedCan–EURACAN clinical practice guidelines for diagnosis, treatment and follow-up, *Ann. Oncol.* 29 (2018) iv79–iv95.
[3] D. Subramaniam, P. Angulo, S. Ponnurangam, et al., Suppressing STAT5 signaling affects osteosarcoma growth and stemness, *Cell Death Dis.* 11 (2) (2020).
[4] B. Yuan, K. Shi, J. Zha, et al., Nuclear receptor modulators inhibit osteosarcoma cell proliferation and tumour growth by regulating the mTOR signaling pathway, *Cell Death Dis.* 14 (1) (2023).
[5] A. Italiano, O. Mir, S. Mathoulin-Pelissier, et al., Cabozantinib in patients with advanced Ewing sarcoma or osteosarcoma (CABONE): a multicentre, single-arm, phase 2 trial, *Lancet Oncol.* 21 (3) (2020) 446–455.
[6] F. Duffaud, O. Mir, P. Boudou-Rouquette, et al., Efficacy and safety of regorafenib in adult patients with metastatic osteosarcoma: a non-comparative,randomised, double-blind, placebo-controlled, phase 2 study, *Lancet Oncol.* 20 (1) (2019) 120–133.
[7] H.A. Tawbi, M. Burgess, V. Bolejack, et al., Pembrolizumab in advanced soft-tissue sarcoma and bone sarcoma (SARC028): a multientre, two-cohort, single-arm, open-label, phase 2 trial, *Lancet Oncol.* 18 (11) (2017) 1493–1501.
[8] L. Xie, J. Xu, X. Sun, et al., Apatinib for advanced osteosarcoma after failure of standard multimodal therapy: an open label phase II clinical trial, *Oncologist* 24 (7) (2019) e542–e550.
[9] S.M. Wilhelm, J. Dumas, L. Adnane, et al., Regorafenib (BAY 73-4506): a new oral multikinase inhibitor of angiogenic, stromal and oncogenic receptor tyrosine kinases with potent preclinical antitumor activity, *Int. J. Cancer* 129 (1) (2011) 245–255.
[10] H. Qian, C. Ji, S. Zhao, et al., Expression and characterization of HSPC129, a RNA polymerase II C-terminal domain phosphatase, *Mol. Cell. Biochem.* 303 (1–2) (2007) 183–188.
[11] Y. Zhao, M. Xiao, B. Sun, et al., C-terminal domain (CTD) small phosphatase-like 2 modulates the canonical bone morphogenetic protein (BMP) signaling and mesenchymal differentiation via Smad dephosphorylation, *J. Biol. Chem.* 289 (38) (2014) 26441–26450.
[12] N. Kang, J. Koo, S. Wang, S.J. Hur, Y.Y. Bahk, A systematic study of nuclear interactome of C-terminal domain small phosphatase-like 2 using inducible expression system and shotgun proteomics, *BMB Rep.* 49 (6) (2016) 319–324.
[13] J. Cao, Y. Yu, Z. Zhang, et al., SCP4 promotes gluconeogenesis through foxO1/3a dephosphorylation, *Diabetes* 67 (1) (2018) 46–57.
[14] Y.-N. Ma, X. Zhang, H.-C. Yu, J.-W. Zhang, CTD small phosphatase like 2 (CTDSPL2) can increase ε- and γ-globin gene expression in K562 cells and CD34+ cells derived from umbilical cord blood, *BMC Cell Biol.* 11 (1) (2010).
[15] Y. Xiao, Y. Chen, A. Peng, J. Dong, The phosphatase CTDSPL2 is phosphorylated in mitosis and a target for restraining tumor growth and motility in pancreatic cancer, *Cancer Lett.* 526 (2022) 53–65.
[16] M. Teufel, H. Seidel, K. Köchert, et al., Biomarkers associated with response to regorafenib in patients with hepatocellular carcinoma, *Gastroenterology* 156 (6) (2019) 1731–1741.
[17] J. Jiang, L. Zhang, H. Chen, et al., Regorafenib induces lethal autophagy arrest by stabilizing PSAT1 in glioblastoma, *Autophagy* 16 (1) (2019) 106–122.
[18] J.-J. Tsai, P.-J. Pan, F.-T. Hsu, Regorafenib induces extrinsic and intrinsic apoptosis through inhibition of ERK/NF-κB activation in hepatocellular carcinoma cells, *Oncol. Rep.* 37 (2) (2017) 1036–1044.
[19] D. Xu, Y. Liu, W. Tang, et al., Regorafenib in refractory metastatic colorectal cancer: a multi-center retrospective study, *Front. Oncol.* 12 (2022).
[20] J. Bruix, S. Qin, P. Merle, et al., Regorafenib for patients with hepatocellular carcinoma who progressed on sorafenib treatment (RESORCE): a randomised, double-blind, placebo-controlled, phase 3 trial, *Lancet* 389 (10064) (2017) 56–66.
[21] D. Doleschel, S. Hoff, S. Koletnik, et al., Regorafenib enhances anti-PD1 immunotherapy efficacy in murine colorectal cancers and their combination prevents tumor regrowth, *J. Exp. Clin. Cancer Res.* 40 (1) (2021).
[22] J. Li, S. Qin, R. Xu, et al., Regorafenib plus best supportive care versus placebo plus best supportive care in Asian patients with previously treated metastatic colorectal cancer (CONCUR): a randomised, double-blind, placebo-controlled, phase 3 trial, *Lancet Oncol.* 16 (6) (2015) 619–629.
[23] A. Grothey, E.V. Cutsem, A. Sobrero, et al., Regorafenib monotherapy for previously treated metastatic colorectal cancer (CORRECT): an international, multicentre, randomised, placebo-controlled, phase 3 trial, *Lancet* 381 (9863) (2013) 303–312.
[24] G.D. Demetri, P. Reichardt, Y.-K. Kang, et al., Efficacy and safety of regorafenib for advanced gastrointestinal stromal tumours after failure of imatinib and sunitinib (GRID): an international, multicentre, randomised, placebo-controlled, phase 3 trial, *Lancet* 381 (9863) (2013) 295–302.
[25] O. Mir, T. Brodowicz, A. Italiano, et al., Safety and efficacy of regorafenib in patients with advanced soft tissue sarcoma (REGOSARC): a randomised, double-blind, placebo-controlled, phase 2 trial, *Lancet Oncol.* 17 (12) (2016) 1732–1742.
[26] Z. Dai, X. Wang, R. Peng, et al., Induction of IL-6Rα by ATF3 enhances IL-6 mediated sorafenib and regorafenib resistance in hepatocellular carcinoma, *Cancer Lett.* 524 (2022) 161–171.
[27] A.F. Shelby Winans, S. Malhotra, V. Balagopal, K.L. Beemon, Integration of ALV into CTDSPL and CTDSPL2 genes in B-cell lymphomas promotes cell immortalization, migration and survival, *Oncotarget* 8 (34) (2017) 57302–57315.
[28] J. Stebbing, L.C. Lit, H. Zhang, et al., The regulatory roles of phosphatases in cancer, *Oncogene* 33 (8) (2013) 939–953.
[29] D.R. Hiroaki Kiyokawa, In vivo roles of CDC25 phosphatases: biological insight into the anti-cancer therapeutic targets, *Anticancer Agents Med Chem.* 8 (8) (2008) 832–836.
[30] L.M. Scott, S.M. Sebti, N.J. Lawrence, J. Wu, targeting protein tyrosine phosphatases for anticancer drug discovery, *Curr. Pharm. Des.* 16 (16) (2010) 1843–1862.